Early therapy with remdesivir and antibody combinations improves COVID-19 disease in mice

David R. Martinez [1, 6, *], Alexandra Schaefer [1, 6], Sarah R. Leist [1], Kendra Gully [1], Joy Y. Feng [2], Elaine Bunyan [2], Danielle P. Porter [2], Tomas Cihlar [2], Stephanie A. Montgomery [3], Ralph S. Baric [1], Michel C. Nussenzweig [4, 5], Timothy P. Sheahan [1, *].

[1] Department of Epidemiology, University of North Carolina at Chapel Hill, Chapel Hill, NC, USA,

[2] Gilead Sciences, Inc, Foster City, CA, USA

[3] Department of Pathology and Laboratory Medicine, University of North Carolina School of Medicine, Chapel Hill, NC, USA,

[4] The Rockefeller University, New York, NY, USA

[5] The Howard Hughes Medical Institute, Chevy Chase, MD, USA

[6] Equal contribution

[*] Correspondence: David R. Martinez, david.rafael.martinez@gmail.com; Timothy P. Sheahan. sheahan@email.unc.edu

KEYWORDS: SARS-CoV-2, remdesivir, RDV, monoclonal antibodies, COVID-19, therapy.

SUMMARY

Improving the standard of clinical care for coronavirus disease 2019 (COVID-19) is a global health priority. Small molecule antivirals like remdesivir (RDV) and biologics such as human monoclonal antibodies (mAb) have demonstrated therapeutic efficacy against SARS-CoV-2, the causative agent of COVID-19. However, the efficacy of single agent therapies has not been comprehensively defined over the time course of infection and it is not known if combination RDV/mAb will improve outcomes over single agent therapies. In kinetic studies in a mouse-adapted SARS-CoV-2 pathogenesis model, we show that single-agent therapies exert potent antiviral effects even when initiated relatively late after infection, but their efficacy is

diminished as a function of time. RDV and a cocktail of two mAbs in combination provided improved outcomes compared to single agents alone extending the therapeutic window of intervention with less weight loss, decreased virus lung titers, reduced acute lung injury, and improved pulmonary function. Overall, we demonstrate that direct-acting antivirals combined with potent mAb can improve outcomes over single agents alone in animal models of COVID-19 thus providing a rationale for the coupling of therapies with disparate modalities to extend the therapeutic window of treatment.

INTRODUCTION

A novel human coronavirus, SARS-CoV-2, emerged in late 2019 in Wuhan, China (Zhou et al., 2020b; Zhu et al., 2020) as the causative agent of coronavirus disease 2019 (COVID-19). The spread of SARS-CoV-2 was explosive with ~100 million confirmed cases and >2 million deaths worldwide as of mid-January 2021. Older individuals and individuals with co-morbidities such as hypertension, cardiovascular disease, and diabetes are at risk for worse COVID-19 clinical outcomes including acute lung injury (ALI), acute respiratory distress syndrome (ARDS), coagulopathies, kidney damage, cardiac and liver disfunction, admission to the intensive care unit, and death (Chen et al., 2020a; Huang et al., 2020; Wang et al., 2020; Xu et al., 2020; Yang et al., 2020). Moreover, long-term COVID-19 symptoms can be debilitating and patients with severe COVID-19 disease can exhibit impaired pulmonary function up to six months post infection (Huang et al., 2021). Therefore, there is a critical need to improve COVID-19 therapies to alleviate disease severity, prevent the most egregious manifestations of pathogenesis, and potentially prevent hospitalization.

Remdesivir (RDV, Veklury) is the only U.S. Food and Drug Administration (FDA) approved small molecule to treat COVID-19. Prior to the emergence of SARS-CoV-2, RDV showed broad-spectrum activity against highly pathogenic human coronaviruses including SARS-CoV, MERS-CoV, and their related enzootic viruses, and endemic common-cold causing coronaviruses (CoV) *in vitro* as well as in various preclinical *in vivo* models of emerging coronavirus disease (Brown et al., 2019; de Wit et al., 2020; Sheahan et al., 2017; Sheahan et al., 2020a). More recently, RDV was shown to exert potent antiviral activity against SARS-CoV-2 *in vitro* (Pruijssers et al., 2020) and therapeutic efficacy in a SARS-CoV-2 rhesus macaque model, which recapitulates mild to moderate respiratory symptomology (Williamson et al., 2020). Collectively, the pre-clinical studies noted above in conjunction with clinical data on RDV administration in healthy volunteers rapidly enabled investigation of RDV in humans with COVID-19 (Humeniuk et al., 2020). In a double-blind, randomized, placebo-controlled trial (ACTT-1), RDV was shown to shorten recovery time in hospitalized COVID-19 patients by 5 days on average as compared to those receiving placebo (Beigel et al., 2020). In contrast, in an open-label, non-placebo-controlled, and non-blinded clinical trial (WHO Solidarity trial) RDV was not shown to improve outcomes in hospitalized patients (2020c). As combinations of RDV with immunomodulators (Baricitinib) have very recently been shown to improve COVID-19 outcomes over single-agent treatment (Kalil et al., 2020), it remains unknown whether RDV combinations with antiviral drugs with complementary modalities will yield similarly promising results.

Several monoclonal antibodies (mAb) targeting the SARS-CoV-2 spike have been shown to potently neutralize SARS-CoV-2 *in vitro* (Jones et al., 2020; Li et al., 2021; Li et al., 2020a; Li et al., 2020b; Robbiani et al., 2020; Rogers et al., 2020; Zost et al., 2020a; Zost et al., 2020b).

Two of the most potent neutralizing mAbs described to date, C144 (IC_{50} = 2.55 ng/mL) and C135 (IC_{50} = = 2.98 ng/mL), were isolated from convalescent human patients and target non-overlapping sites on the receptor binding domain (RBD) on the SARS-CoV-2 spike protein (Barnes et al., 2020a; Barnes et al., 2020b; Robbiani et al., 2020; Schäfer et al., 2021). C144 can bind to the "down" and "up" RBD positions and has a quaternary epitope that requires contact with two adjacent RBDs, effectively preventing the binding of the SARS-CoV-2 trimeric spike from unfolding and binding ACE2, whereas C135 binds to the RBD outside the ACE2 binding site (Barnes et al., 2020a). Similar to the antiviral efficacy of RDV, monoclonal antibody (mAb) drugs targeting the SARS-CoV-2 spike glycoprotein have demonstrated therapeutic efficacy in multiple pre-clinical models of viral pathogenesis, and a select few have been authorized for emergency use by the FDA to treat COVID-19 (2020a; Barnes et al., 2020a; Barnes et al., 2020b; Jones et al., 2020; Schäfer et al., 2021). As a result of their early promise in pre-clinical settings, human clinical trials were initiated to examine the therapeutic efficacy of SARS-CoV-2 mAbs in infected patients (Chen et al., 2020b; Weinreich et al., 2020). Despite the clear prophylactic benefit of mAbs, the optimal timing of therapeutic mAb treatment is unclear. In fact, a recent study in hospitalized patients with more severe COVID-19 symptoms who received RDV and Ly-CoV555 mAb did not show substantial benefit (2020b). Therefore, it is not known if combination therapy of different antivirals, such as RDV and neutralizing mAbs, in mild or non-severe COVID-19 infections will lead to a more rapid improvement in outpatient settings and early in the course of disease. Thus, a key question in the field is: what is the critical window of intervention with antivirals? The answer is of particular importance, as an understanding of the preferred time to treat with antivirals may help to optimize the benefit of RDV previously shown in recent human clinical trials in hospitalized patients (Beigel et al., 2020).

Here, in a robust mouse model of severe SARS-CoV-2 pathogenesis (SARS-CoV-2 MA10), we define the prophylactic and therapeutic efficacy of RDV and mAbs used singly and in combination. We show that the prophylactic and early therapeutic administration of RDV or mAb can prevent severe COVID-19 disease symptoms in SARS-CoV-2 MA10-infected mice. Importantly, we show that combination therapy administered at later times during the course of infection improved outcomes compared to either monotherapy thus extending the therapeutic window within which outcomes can be improved. Our data provide the scientific rationale supporting the investigation of RDV and mAb combination therapy in humans with COVID-19.

RESULTS

Prophylactic and therapeutic RDV protect against COVID-19 disease in mice.

Due to a serum esterase in mice that dramatically reduces RDV stability (carboxyesterase 1c (*Ces1c*)), we performed all of our RDV efficacy studies in C57BL/6 mice lacking this gene (*Ces1c*$^{(-/-)}$) (Sheahan et al., 2017). Although we had previously explored the *in vivo* efficacy of RDV against SARS-CoV/SARS-CoV-2 chimeric viruses (Pruijssers et al., 2020), we had not yet evaluated RDV in mice infected with our recently described mouse adapted SARS-CoV-2 (SARS-CoV-2 MA10) (Leist et al., 2020). We initiated twice-daily treatment of mice with a human equivalent dose of RDV (25mg/kg) or vehicle -12 hours prior to infection or +12 (early), 24 (mid-late), or 48 (late) hours post infection (hpi) with 1×10^4 particle forming units (PFU) of SARS-CoV-2 MA10. Body weight loss is a crude marker of emerging coronavirus pathogenesis. Unlike the rapid and uniform weight loss observed in mice administered vehicle, body weight loss was prevented with prophylactic RDV treatment (Figure 1A). When initiated after SARS-

CoV-2 infection, only early therapeutic intervention (+12hr) was able to significantly diminish weight loss (Figure 1A). While RDV therapy initiated at 24hr could not prevent weight loss, lung viral load was significantly diminished in this group similar to those receiving prophylaxis (-12hr) or early therapeutic intervention (+12hr) (Figure 1B). Similarly, lung pathological features, such as lung discoloration which is characteristic of severe lung damage observed in the vehicle-treated animals, were diminished in all treatment groups except those where RDV was initiated 48hpi (Figure 1C). Lung discoloration is the gross manifestation of various processes of acute lung damage, including but not limited to congestion, edema, and protein exudation. The American Thoracic Society (ATS) created a tool (Matute-Bello lung pathology score) to quantitate the pathological features of ALI in the mouse lung which has recently been employed to describe the pulmonary pathogenesis in BALB/c mice infected with SARS-CoV-2 MA10 (Leist et al., 2020; Matute-Bello et al., 2011). Using this tool, three random diseased fields in lung tissue sections per mouse were blindly evaluated by a board-certified pathologist revealing that RDV prophylaxis and therapy at +12 and +24 hpi reduced ALI as compared to vehicle treated animals (Figure 1D). With a complementary histological tool, we similarly scored lung tissue sections for diffuse alveolar damage (DAD) (Figure 1E), the pathological hallmark of ALI (cellular sloughing, necrosis, hyaline membranes, etc.) (Schmidt et al., 2018; Sheahan et al., 2020a) and found these data were consistent with those in Figure 1D. Lastly, pulmonary function was measured daily in a subset of mice per group (N = 4) by whole-body plethysmography (WBP). As shown with the WBP metric PenH, a metric for airway resistance or obstruction (Sheahan et al., 2017), only prophylactic and early therapeutic intervention (+12hpi) with RDV could prevent the loss of pulmonary function observed in the other treatment groups and vehicle. Together, these data show that prophylactic and therapeutic RDV administered prior to peak

virus replication in the lung (48hpi) can not only robustly exert an antiviral effect but also can significantly reduce COVID-19 symptomology.

Prophylactic and therapeutic mAbs reduce SARS-CoV-2 pathogenesis.

While the therapeutic efficacy of mAbs against SARS-CoV-2 has been shown in hamsters and rhesus macaques (2020b; Baum et al., 2020; Jones et al., 2020; Rogers et al., 2020; Schäfer et al., 2021), recent studies reported little benefit in hospitalized patients with advanced COVID-19 disease (2020b; Chen et al., 2020b). In COVID-19 patients with clear onset of symptoms, the turning point in treatment initiation when mAbs lose their therapeutic effect remains unknown. To address this, we determined the prophylactic and therapeutic efficacy of two potent neutralizing monoclonal antibodies, C144 and C135, singly and in combination in the SARS-CoV-2 MA10 pathogenesis model noted above. We treated C57BL/6 mice with a single dose of single or combination mAb 12hr prior to or 12, 24, or 48hr after infection with 1×10^4 PFU of SARS-CoV-2 MA10. Mice treated prophylactically 12 hours before infection with C144 alone, C135 alone, or a combination of C144 + C135 were protected against bodyweight loss and lung viral replication measured at day 5 post infection (d5pi) (Figure S1A, Figure S1B, Figure 2A, and Figure S2B). Lung pathology as measured by lung discoloration, and two independent lung pathology scoring systems demonstrated complete protection from lung pathology in animals treated with C144 + C135 and in the C135 alone group, whereas negative control HIV mAb treated animals exhibited severe lung pathology (Figure 2C, 2D, 2E and Figure S1C-E, S6).

We then evaluated the early (12hpi), mid-late (24hpi), and late (48hpi) therapeutic efficacy of either combinations of these monoclonal antibodies or as single agents in infected mice. Mice that received therapeutic treatment of the C144 + C135 and the mAbs as single

agents at 12 and 24hpi were protected against bodyweight loss and lung viral replication compared to mice treated with HIV mAb (Figure 2A, Figure 2B, Figure S2A, S2B, S3A, and S3B). Little protection against bodyweight loss was observed in the 48hpi treatment group (Figure 2A and Figure S4A). In contrast, to the C144 + C135 and to the C135 single agent, mice treated prophylactically and therapeutically at +12, 24, and 48hpi with C144 had low lung viral titer levels (Figure S1B), likely due to a Q493K spike mutation that enabled that mouse-adaption of SARS-CoV-2 and this amino acid residue is important for the binding of C144 (Barnes et al., 2020a; Barnes et al., 2020b; Gaebler et al., 2021; Leist et al., 2020). We also observed treatment initiation time-dependent protection from lung discoloration with the most protection in the C144 + C135 group and little to no benefit in the single agent mAb treatments at 48hpi (Figure 2C, Figures S2C, S3C, S4C, and S6). We again employed the Matute-Bello and DAD lung pathology scoring tools to quantitate ALI in the different therapy groups. We observed the most protection from ALI in the C144 + C135 group early in the course of disease, whereas little to no protection was observed in the single mAb groups at 24 and 48hpi (Figure 2D 2E, Figure S2D, S2E, S3D, S3E, S4D, and S4E). As shown with the WBP metric PenH, prophylactic and early therapeutic intervention (+12hpi) with C144 + C135 fully prevented the loss of pulmonary function compared to vehicle, with some small benefit at 24hpi (Figure 2F). Thus, mAb treatment before peak lung viral replication, which is at 48hpi in this mouse model (Leist et al., 2020), significantly reduces COVID-19 symptomology.

Combination RDV and mAb therapy improves multiple outcomes when initiated at 24hpi.

Since treatment with RDV or C144 + C135 mAb treatment failed to improve outcomes when administered later in infection, we sought to determine if the co-administration of RDV

and C144 + C135 could extend the therapeutic window and show clinical benefit where single agents failed. We first performed an efficacy study initiating combination therapy 24hr post infection where both single agents failed to prevent loss of pulmonary function. Here we assessed the following groups: 1) vehicle + HIV mAb (vehicle/control mAb), 2) vehicle + C144 + C135 (vehicle/mAb), 3) RDV + HIV mAb (RDV/control mAb), 4) RDV + C144 + C135 (RDV/mAb). While single agents provided some benefit in reducing bodyweight loss, only the RDV/mAb combination consistently reduced weight loss between d4 and d6pi (Figure 3A). By d4pi, RDV/mAb combination-treated group retained the highest % starting bodyweight compared to either the vehicle/control mAb-, the vehicle/mAb-, or RDV/control mAb-treated groups. Both the vehicle/mAb- and RDV/control mAb-treated groups showed improvement at d4-7pi compared to the vehicle/control mAb-treated group albeit it was not as robust as the RDV/mAb combination-treated group (Figure 3A). Forty percent of vehicle/control mAb treated animals succumbed to SARS-CoV-2 disease whereas all other groups survived throughout the experiment (Figure 3B). While we observed some protection against lung discoloration in both the vehicle/mAb- and RDV/control mAb-treated groups, we observed the lowest lung discoloration in the RDV/mAb combination-treated group (Figure 3C). WBP metric PenH showed that RDV/mAb combination-treated group had marked improvement in pulmonary function by d3pi and through d5pi (Figure 3E). Notably, we did not observe a significant improvement in pulmonary function in the 24hpi RDV alone-treated group (Figure 1F) and did not observe an improvement in pulmonary function until d5pi in the 24hpi C144 + C135-treated group (Figure 2F). In summary, the combination of RDV with mAbs leads to improvement in metrics of COVID-19 disease in this stringent SARS-CoV-2 mouse pathogenesis model.

Combination RDV/mAb cocktail extends the therapeutic window over single agent therapy

As RDV/mAb combination therapy exerted notable improvements in outcomes when initiating treatment 24hpi, we sought to determine if this regimen could improve outcomes at later times. In studies similar to the design in Figure 3, we initiated treatment 36hr after infection with 1×10^4 PFU SARS-CoV-2 MA10 in C57BL/6 (*Ces1c* $^{(-/-)}$) mice. Notably, we observed the most significant benefit in groups that received RDV/mAb combination. RDV/mAb combination-treated groups had the most significant protection against bodyweight loss on 4dpi and 5dpi compared to the vehicle/control mAb group (Figure 4A). By 3dpi, only the RDV/control mAb and RDV/mAb-treated groups had lower lung viral titers compared to the vehicle/control mAb-treated group (Figure 4B). While a few of the RDV/control mAb-treated mice had measurable virus in the lung on 5dpi, virus was not detected in lung tissue from mice treated with vehicle/mAb or RDV/mAb (Figure 4C). Remarkably, the RDV/mAb combination group also exhibited the lowest lung discoloration and lung pathology, the Matute-Bello and DAD lung pathology scoring tools, compared to the vehicle/mAb- and RDV/control mAb-treated groups (Figure 4D, 4E, 4F). Finally, the treatment with RDV/mAb reduced the loss of pulmonary function 3 to 5dpi as compared to vehicle/control mAb treatment (Figure 4G). Altogether, our findings demonstrate that the combination of two direct antivirals, RDV and potent neutralizing mAbs, can extend the window of intervention and lead to improved disease symptoms of COVID-19 in a robust animal model of SARS-CoV-2 pathogenesis.

DISCUSSION

RDV is a broad-spectrum antiviral drug and has therapeutic efficacy against multiple emerging CoVs in various pre-clinical models (Agostini et al., 2018; Brown et al., 2019; de Wit

et al., 2020; Sheahan et al., 2017). In addition to the *in vitro* activity of RDV against SARS-CoV-2 in early 2020 (Pruijssers et al., 2020), RDV can exert an antiviral effect and diminish SARS-CoV-2 disease in rhesus macaques which develop mild respiratory disease (Williamson et al., 2020). This study offers the first evaluation of RDV against SARS-CoV-2 in a stringent animal model of SARS-CoV-2 disease that recapitulates several aspects of severe human COVID-19. Importantly, the robust protection against SARS-CoV-2 disease described herein is consistent with the antiviral effect of RDV against related coronaviruses.

Similar to the efficacy results in pre-clinical models (Jones et al., 2020), neutralizing monoclonal antibody treatment with LY-CoV555 and LY-CoV016 in outpatients with mild or moderate COVID-19 led to a significant reduction in viral load in load in nasopharyngeal swabs (Gottlieb et al., 2021). In agreement, a monoclonal antibody cocktail developed by Regeneron, REGN-COV2, also showed a reduction in viral load in outpatients (Weinreich et al., 2020). Given the early promise of neutralizing monoclonal antibodies in outpatient settings, the FDA issued Emergency Use Authorization (EUA) to Eli Lilly's LY-CoV555 for use in recently diagnosed patients with mild COVID-19 disease symptoms and who are at risk for progressing to severe disease (2020a). However, hospitalized patients with advanced COVID-19 disease treated with LY-CoV555 and RDV did not have measurably improved clinical outcomes compared to patients that received the standard of care (2020b). It should also be noted that the failure of LY-CoV555 administered late in the course of COVID-19 is similar to the late failures of antivirals reported in the setting of the influenza antivirals, such as Tamiflu, in hospitalized patients (Muthuri et al., 2014), in that early antiviral intervention offers the most clinical benefit. Like mouse-adapted models of SARS-CoV and MERS-CoV, the replication kinetics of mouse-adapted SARS-CoV-2 MA10 in mice is compressed as compared to that of SARS-CoV-2 in

humans with peak virus replication occurring in the mouse at 48 hours post infection (Leist et al., 2020). In contrast, the replication kinetics of SARS-CoV-2 in the airways of infected humans is more variable with reports estimating peak replication within the first week after the onset of symptoms (Liu et al., 2020; Zheng et al., 2020). Moreover, human patients can shed viral RNA in the mucosa of the upper respiratory tract as long as 24 days post infection (Zhou et al., 2020a), underlining that humans sustain viral replication and symptoms of COVID-19 longer than mice. Thus, the window within which to intervene with antiviral therapy prior to the peak of virus replication in humans is dramatically different than in a mouse (~2 days). This is supported by the fact that neither RDV nor mAb therapy could improve outcomes if administered concurrent with peak replication in the mouse lung. Moreover, our mouse model data is in step with the clinical trial findings of RDV and mAbs in that antiviral activity performance and clinical outcomes are improved with earlier treatment with RDV or mAbs.

SARS-CoV-2 spike mutations can be selected by single mAb therapies but are less likely to arise in the setting of combinations of monoclonal antibodies with distinct epitope specificities (Weisblum et al., 2020). As SARS-CoV-2 continues to evolve, mutations may arise in spike that alter mAb binding epitopes and diminish their therapeutic potential. With the emergence of spike variants that contain mutations K417N, Y453F, S477R, N501Y, D614G, and R683G and the increased resistance of these variants to mAbs (Wang et al., 2021), the use of RDV/mAb will be critically important to avoid further selection of escape variants and for a more potent antiviral therapy. Furthermore, the use of RDV/mAb combination therapy could also be deployed in the settings of immunocompromised patients with prolonged viral shedding (Choi et al., 2020) as well as in settings where the virus may develop mutations in the RNA-dependent RNA polymerase that modulate resistance to RDV therapy (Martinot et al., 2020). Thus, in the context

of monotherapy, the combination of a polymerase-targeting drug like RDV used in combination with either a single mAb or a two-mAb cocktail may be a more effective tool to prevent the selection of variants that are resistant to monotherapies. Combination therapies comprised of antivirals with disparate and complementary mechanisms of action, like RDV and mAbs, has the potential to improve outcomes if given early enough in the disease course even if circulating strains carry mutations that may negatively impact one component of the regimen.

Although our study demonstrates that the combination of RDV and mAbs lead to more rapid recovery from disease in mice, a clear downside is that both RDV and mAbs are generally administered as intravenous treatments which is not a practical method for broad human distribution. Potential strategies to allow the wider dissemination of treatment may include subcutaneous or intramuscular administration of mAbs, which may aid in the more rapid distribution of antiviral treatments in an outpatient setting that can protect against SARS-CoV-2 acquisition. Given the improved efficacy of RDV/mAb combination therapy, it will also be critical to develop next-generation antivirals that can be administered orally, which could be more easily combined with mAbs in an outpatient setting, potentially to complement other oral direct-acting antivirals (Sheahan et al., 2020b). As coronaviruses have consistently emerged in the last two decades, and genetically distinct and pathogenic coronaviruses are likely to continue to emerge, refining combination therapies, such as oral antivirals and combinations of mAbs, will better prepare us to combat future coronavirus outbreaks. Altogether, our findings provide the rationale that the combination of broadly neutralizing mAbs against Sarbecoviruses in combination with broad-acting antivirals may be a useful strategy to mitigate future outbreaks with emerging coronaviruses. Our results demonstrate that RDV and neutralizing mAb treatments late in infection offer little benefit in the SARS-CoV-2 mouse model and with regard

to therapeutic use in humans raise the hypotheses that 1) early treatment with direct antivirals and 2) combination therapy with direct-acting antivirals in the early course of COVID-19 will improve outcomes in humans.

STAR METHODS

Lead Contact

Further information and requests for resources and reagents should be directed to and will be fulfilled by the Lead Contact, Timothy P. Sheahan (sheahan@email.unc.edu)

Materials Availability

Not applicable.

Data and Code availability.

Not applicable.

EXPERIMENTAL MODEL AND SUBJECT DETAILS

Animals and virus infections

Twenty-week-old male and female *Ces1c* $^{(-/-)}$ on a B6 background (C57BL/6J: Jackson Laboratory # 014096) were purchased from Jackson Laboratory. A mouse-adapted SARS-CoV-2 virus (MA10) was used in all experiments and this virus was previously described (Leist et al., 2020). Briefly, mutations predictive of increased affinity to mouse ACE2 were introduced into a SARS-CoV-2 virus plasmid system and the virus was recovered by reverse genetics (Dinnon et al., 2020). This modified virus was then serially passaged in aged BALBc mice (Envigo #047)

for ten passages which we refer to as the mouse-adapted passage 10 (MA10) SARS-CoV-2 (Leist et al., 2020). All mice were anesthetized and infected with SARS-CoV-2 MA10 intranasally with 1×10^4 PFU/ml. Mice were weighed daily and were monitored for signs of SARS-CoV-2 clinical disease in all experiments.

Animal care

The study was carried out in accordance with the recommendations for care and use of animals by the Office of Laboratory Animal Welfare (OLAW), National Institutes of Health and the Institutional Animal Care and Use Committee (IACUC) protocol number: 20-059 at University of North Carolina (UNC permit no. A-3410-01). Virus inoculations were performed under anesthesia and all efforts were made to minimize animal suffering. Animals were housed in groups and fed standard chow diets.

METHOD DETAILS

Study design and treatment groups

For the RDV experiment, a total of N=40, ~20-week-old male and female mice were divided into four groups each with N=10 mice with equal numbers of females and males in each group. RDV was administered subcutaneously twice per day (BID) at 25 mg/kg. Groups of N=10 mice (N=5 males and N=5 females) were used in either the prophylaxis -12 hours before infection group, the early therapeutic 12 hours post infection group, the mid-late therapeutic 24 hours post infection group, and the late therapeutic 48 hours post infection group.

For the initial monoclonal antibody experiment, mice were infected as described above and weighed daily and were monitored for signs of SARS-CoV-2 clinical disease. A total amount of 200 μg of C144 + C135, 200 μg of C144, 200 μg of C135, and 200 μg of HIV mAbs 3BC117 + 10-1074 was administered intraperitonially once by injection for each intervention group. Groups of N=20 female mice (N=5 mice treated with C144 + C135, N=5 mice treated with C144, N=5 mice treated with C135, and N=5 mice treated with 3BNC117 + 10-1074) were administered antibody 12 hours before infection, N=20 female mice (N=5 mice treated with C144 + C135, N=5 mice treated with C144, N=5 mice treated with C135, and N=5 mice treated with 3BNC117 + 10-1074) were administered antibody 12hpi (early therapeutic group), N=20 female mice (N=5 mice treated with C144 + C135, N=5 mice treated with C144, N=5 mice treated with C135, and N=5 mice treated with 3BNC117 + 10-1074) were administered antibody 24hpi (mid-late therapeutic group), and N=20 female mice (N=5 mice treated with C144 + C135, N=5 mice treated with C144, N=5 mice treated with C135, and N=5 mice treated with 3BNC117 + 10-1074) were administered antibody 48hpi (late therapeutic group).

For the 24hpi drug and mAb combination intervention experiment, a total of N=40, ~20-week-old male and female mice were divided into four groups each with N=10 mice with equal numbers of females and males in each group. At 24hpi, RDV treatment was initiated by subcutaneous injection twice per day (BID) at 25 mg/kg, and a total amount of 200 μg of C144 + C135 was administered intraperitonially once by injection. N=10 mice (N=5 males and N=5 females) were used in the vehicle + HIV mAb group. N=10 mice (N=5 males and N=5 females) were used in the vehicle + C144 + C135 mAb group. N=10 mice (N=5 males and N=5 females) were used in the RDV + HIV mAb group. N=10 mice (N=5 males and N=5 females) were used in the RDV + C144 + C135 mAb group.

For the 36hpi drug + mAb combination intervention experiment, a total of N=64, ~20-week-old male and female mice were divided into four groups each with N=16 mice with an equal number of females and males in each group. At 36hpi, RDV treatment was initiated by subcutaneous injection twice per day (BID) at 25 mg/kg, and a total of 200 μg of each monoclonal antibody treatment was administered intraperitonially once by injection. N=32 mice were harvested at d3pi to evaluate early lung viral replication titers, and remaining mice were harvested at d5pi. N=16 mice (N=8 males and N=8 females) were used in the vehicle + HIV mAb group. N=16 mice (N=8 males and N=8 females) were used in the vehicle + C144 + C135 mAb group. N=16 mice (N=8 males and N=8 females) were used in the RDV + HIV mAb group. N=16 mice (N=8 males and N=8 females) were used in the RDV + C144 + C135 mAb group.

Lung pathology scoring

Acute lung injury was quantified via two separate lung pathology scoring scales: Matute-Bello and Diffuse Alveolar Damage (DAD) scoring systems. Analyses and scoring were performed by a Board Certified Veterinary Pathologist who was blinded to the treatment groups as described previously (Sheahan et al., 2020a). Lung pathology slides were read and scored at 600X total magnification.

The lung injury scoring system used is from the American Thoracic Society (Matute-Bello) in order to help quantitate histological features of ALI observed in mouse models to relate this injury to human settings. In a blinded manner, three random fields of lung tissue were chosen and scored for the following: (A) neutrophils in the alveolar space (none = 0, 1–5 cells = 1, > 5 cells = 2), (B) neutrophils in the interstitial septae (none = 0, 1–5 cells = 1, > 5 cells = 2), (C) hyaline membranes (none = 0, one membrane = 1, > 1 membrane = 2), (D) Proteinaceous

debris in air spaces (none = 0, one instance = 1, > 1 instance = 2), (E) alveolar septal thickening (< 2x mock thickness = 0, 2–4x mock thickness = 1, > 4x mock thickness = 2). To obtain a lung injury score per field, A–E scores were put into the following formula score = [(20x A) + (14 x B) + (7 x C) + (7 x D) + (2 x E)]/100. This formula contains multipliers that assign varying levels of importance for each phenotype of the disease state. The scores for the three fields per mouse were averaged to obtain a final score ranging from 0 to and including 1.

The second histology scoring scale to quantify acute lung injury was adopted from a lung pathology scoring system from lung RSV infection in mice (Schmidt et al., 2018). This lung histology scoring scale measures diffuse alveolar damage (DAD). Similar to the implementation of the ATS histology scoring scale, three random fields of lung tissue were scored for the following in a blinded manner: 1= absence of cellular sloughing and necrosis, 2=Uncommon solitary cell sloughing and necrosis (1–2 foci/field), 3=multifocal (3+foci) cellular sloughing and necrosis with uncommon septal wall hyalinization, or 4=multifocal (>75% of field) cellular sloughing and necrosis with common and/or prominent hyaline membranes. The scores for the three fields per mouse were averaged to get a final DAD score per mouse. The microscope images were generated using an Olympus Bx43 light microscope and CellSense Entry v3.1 software.

Remdesivir (RDV)

RDV was synthesized at Gilead Inc., and its chemical composition and purity were analyzed by nuclear magnetic resonance, high resolution mass spectrometry, and high-performance liquid chromatography. RDV was solubilized in 12% sulfobutylether-β-cyclodextrin in water (with HCl/NaOH) at pH 5 for *in vivo* studies in mice. RDV was made

available to UNC Chapel Hill under an existing material transfer agreement with Gilead Sciences Inc.

Biocontainment and biosafety

Studies were approved by the UNC Institutional Biosafety Committee approved by animal and experimental protocols in the Baric laboratory. All work described here was performed with approved standard operating procedures for SARS-CoV-2 in a biosafety level 3 (BSL-3) facility conforming to requirements recommended in the Microbiological and Biomedical Laboratories, by the U.S. Department of Health and Human Service, the U.S. Public Health Service, and the U.S. Center for Disease Control and Prevention (CDC), and the National Institutes of Health (NIH).

Statistics

All statistical analyses were performed using GraphPad Prism 9. Statistical tests used in each figure are denoted in the corresponding figure legend.

Acknowledgements

David R. Martinez is funded by an NIH F32 AI152296, a Burroughs Wellcome Fund Postdoctoral Enrichment Program Award, and was supported by an NIH NIAID T32 AI007151. This work was supported by NIAID R01 AI132178 awarded to Timothy P. Sheahan and Ralph S. Baric, and an NIH animal models contract (HHSN272201700036I) to R.S.B. This project was also supported by the North Carolina Policy Collaboratory at the University of North Carolina at Chapel Hill with funding from the North Carolina Coronavirus Relief Fund established and

appropriated by the North Carolina General Assembly. Michel C. Nussenzweig is an investigator of the Howard Hughes Medical Institute. Animal histopathology services were performed by the Animal Histopathology & Laboratory Medicine Core at the University of North Carolina, which is supported in part by an NCI Center Core Support Grant (5P30CA016086-41) to the UNC Lineberger Comprehensive Cancer Center.

Author contributions

Conceived the study: D.R.M, A.S., R.S.B, M.C.N., and T.P.S. Designed experiments: D.R.M, A.S., J.Y.F., E.B., D.P.P., T.C., R.S.B, M.C.N., and T.P.S. Performed laboratory experiments: D.R.M, A.S., S.R. L., K.G., T.P.S.; Provided critical reagents: J.Y.F., E.B., D.P.P., T.C.; Wrote the first draft of the paper: D.R.M and T.P.S. Edited the manuscript: D.R.M, A.S., S.R. L., K.G., J.Y.F., E.B., D.P.P., T.C., S.A.M., R.S.B, M.C.N., and T.P.S. All authors reviewed and approved the manuscript.

Conflict of interest

J.Y.F., E.B., D.P.P., T.C. are employed by Gilead Sciences Inc.

REFERENCES

(2020a). An EUA for Bamlanivimab—A Monoclonal Antibody for COVID-19. JAMA.

(2020b). A Neutralizing Monoclonal Antibody for Hospitalized Patients with Covid-19. New England Journal of Medicine.

(2020c). Repurposed Antiviral Drugs for Covid-19 — Interim WHO Solidarity Trial Results. New England Journal of Medicine.

Agostini, M.L., Andres, E.L., Sims, A.C., Graham, R.L., Sheahan, T.P., Lu, X., Smith, E.C., Case, J.B., Feng, J.Y., Jordan, R., *et al.* (2018). Coronavirus Susceptibility to the Antiviral Remdesivir (GS-5734) Is Mediated by the Viral Polymerase and the Proofreading Exoribonuclease. mBio *9*.

Barnes, C.O., Jette, C.A., Abernathy, M.E., Dam, K.A., Esswein, S.R., Gristick, H.B., Malyutin, A.G., Sharaf, N.G., Huey-Tubman, K.E., Lee, Y.E., *et al.* (2020a). SARS-CoV-2 neutralizing antibody structures inform therapeutic strategies. Nature *588*, 682-687.

Barnes, C.O., West, A.P., Jr., Huey-Tubman, K.E., Hoffmann, M.A.G., Sharaf, N.G., Hoffman, P.R., Koranda, N., Gristick, H.B., Gaebler, C., Muecksch, F., *et al.* (2020b). Structures of Human Antibodies Bound to SARS-CoV-2 Spike Reveal Common Epitopes and Recurrent Features of Antibodies. Cell *182*, 828-842.e816.

Baum, A., Ajithdoss, D., Copin, R., Zhou, A., Lanza, K., Negron, N., Ni, M., Wei, Y., Mohammadi, K., Musser, B., *et al.* (2020). REGN-COV2 antibodies prevent and treat SARS-CoV-2 infection in rhesus macaques and hamsters. Science *370*, 1110-1115.

Beigel, J.H., Tomashek, K.M., Dodd, L.E., Mehta, A.K., Zingman, B.S., Kalil, A.C., Hohmann, E., Chu, H.Y., Luetkemeyer, A., Kline, S., *et al.* (2020). Remdesivir for the Treatment of Covid-19 — Final Report. New England Journal of Medicine *383*, 1813-1826.

Brown, A.J., Won, J.J., Graham, R.L., Dinnon, K.H., 3rd, Sims, A.C., Feng, J.Y., Cihlar, T., Denison, M.R., Baric, R.S., and Sheahan, T.P. (2019). Broad spectrum antiviral remdesivir inhibits human endemic and zoonotic deltacoronaviruses with a highly divergent RNA dependent RNA polymerase. Antiviral Res *169*, 104541.

Chen, N., Zhou, M., Dong, X., Qu, J., Gong, F., Han, Y., Qiu, Y., Wang, J., Liu, Y., Wei, Y., *et al*. (2020a). Epidemiological and clinical characteristics of 99 cases of 2019 novel coronavirus pneumonia in Wuhan, China: a descriptive study. Lancet *395*, 507-513.

Chen, P., Nirula, A., Heller, B., Gottlieb, R.L., Boscia, J., Morris, J., Huhn, G., Cardona, J., Mocherla, B., Stosor, V., *et al.* (2020b). SARS-CoV-2 Neutralizing Antibody LY-CoV555 in Outpatients with Covid-19. N Engl J Med.

Choi, B., Choudhary, M.C., Regan, J., Sparks, J.A., Padera, R.F., Qiu, X., Solomon, I.H., Kuo, H.-H., Boucau, J., Bowman, K., *et al.* (2020). Persistence and Evolution of SARS-CoV-2 in an Immunocompromised Host. New England Journal of Medicine *383*, 2291-2293.

de Wit, E., Feldmann, F., Cronin, J., Jordan, R., Okumura, A., Thomas, T., Scott, D., Cihlar, T., and Feldmann, H. (2020). Prophylactic and therapeutic remdesivir (GS-5734) treatment in the rhesus macaque model of MERS-CoV infection. Proc Natl Acad Sci U S A *117*, 6771-6776.

Dinnon, K.H., 3rd, Leist, S.R., Schafer, A., Edwards, C.E., Martinez, D.R., Montgomery, S.A., West, A., Yount, B.L., Jr., Hou, Y.J., Adams, L.E., *et al.* (2020). A mouse-adapted model of SARS-CoV-2 to test COVID-19 countermeasures. Nature *586*, 560-566.

Gaebler, C., Wang, Z., Lorenzi, J.C.C., Muecksch, F., Finkin, S., Tokuyama, M., Cho, A., Jankovic, M., Schaefer-Babajew, D., Oliveira, T.Y., *et al.* (2021). Evolution of antibody immunity to SARS-CoV-2. Nature.

Gottlieb, R.L., Nirula, A., Chen, P., Boscia, J., Heller, B., Morris, J., Huhn, G., Cardona, J., Mocherla, B., Stosor, V., *et al.* (2021). Effect of Bamlanivimab as Monotherapy or in Combination With Etesevimab on Viral Load in Patients With Mild to Moderate COVID-19: A Randomized Clinical Trial. Jama.

Huang, C., Huang, L., Wang, Y., Li, X., Ren, L., Gu, X., Kang, L., Guo, L., Liu, M., Zhou, X., *et al.* (2021). 6-month consequences of COVID-19 in patients discharged from hospital: a cohort study. Lancet.

Huang, C., Wang, Y., Li, X., Ren, L., Zhao, J., Hu, Y., Zhang, L., Fan, G., Xu, J., Gu, X., *et al.* (2020). Clinical features of patients infected with 2019 novel coronavirus in Wuhan, China. Lancet *395*, 497-506.

Humeniuk, R., Mathias, A., Cao, H., Osinusi, A., Shen, G., Chng, E., Ling, J., Vu, A., and German, P. (2020). Safety, Tolerability, and Pharmacokinetics of Remdesivir, An Antiviral for Treatment of COVID-19, in Healthy Subjects. Clin Transl Sci *13*, 896-906.

Jones, B.E., Brown-Augsburger, P.L., Corbett, K.S., Westendorf, K., Davies, J., Cujec, T.P., Wiethoff, C.M., Blackbourne, J.L., Heinz, B.A., Foster, D., *et al.* (2020). LY-CoV555, a rapidly isolated potent neutralizing antibody, provides protection in a non-human primate model of SARS-CoV-2 infection. bioRxiv.

Kalil, A.C., Patterson, T.F., Mehta, A.K., Tomashek, K.M., Wolfe, C.R., Ghazaryan, V., Marconi, V.C., Ruiz-Palacios, G.M., Hsieh, L., Kline, S., *et al.* (2020). Baricitinib plus Remdesivir for Hospitalized Adults with Covid-19. New England Journal of Medicine.

Leist, S.R., Dinnon, K.H., 3rd, Schäfer, A., Tse, L.V., Okuda, K., Hou, Y.J., West, A., Edwards, C.E., Sanders, W., Fritch, E.J., *et al.* (2020). A Mouse-Adapted SARS-CoV-2 Induces Acute Lung Injury and Mortality in Standard Laboratory Mice. Cell *183*, 1070-1085.e1012.

Li, D., Edwards, R.J., Manne, K., Martinez, D.R., Schäfer, A., Alam, S.M., Wiehe, K., Lu, X., Parks, R., Sutherland, L.L., *et al.* (2021). The functions of SARS-CoV-2 neutralizing and infection-enhancing antibodies in vitro and in mice and nonhuman primates. bioRxiv.

Li, W., Chen, C., Drelich, A., Martinez, D.R., Gralinski, L.E., Sun, Z., Schäfer, A., Kulkarni, S.S., Liu, X., Leist, S.R., *et al.* (2020a). Rapid identification of a human antibody with high prophylactic and therapeutic efficacy in three animal models of SARS-CoV-2 infection. Proc Natl Acad Sci U S A *117*, 29832-29838.

Li, W., Schäfer, A., Kulkarni, S.S., Liu, X., Martinez, D.R., Chen, C., Sun, Z., Leist, S.R., Drelich, A., Zhang, L., *et al.* (2020b). High Potency of a Bivalent Human V(H) Domain in SARS-CoV-2 Animal Models. Cell *183*, 429-441.e416.

Liu, Y., Yan, L.M., Wan, L., Xiang, T.X., Le, A., Liu, J.M., Peiris, M., Poon, L.L.M., and Zhang, W. (2020). Viral dynamics in mild and severe cases of COVID-19. Lancet Infect Dis *20*, 656-657.

Martinot, M., Jary, A., Fafi-Kremer, S., Leducq, V., Delagreverie, H., Garnier, M., Pacanowski, J., Mékinian, A., Pirenne, F., Tiberghien, P., *et al.* (2020). Remdesivir failure with SARS-CoV-2 RNA-dependent RNA-polymerase mutation in a B-cell immunodeficient patient with protracted Covid-19. Clin Infect Dis.

Matute-Bello, G., Downey, G., Moore, B.B., Groshong, S.D., Matthay, M.A., Slutsky, A.S., and Kuebler, W.M. (2011). An official American Thoracic Society workshop report: features and measurements of experimental acute lung injury in animals. Am J Respir Cell Mol Biol *44*, 725-738.

Muthuri, S.G., Venkatesan, S., Myles, P.R., Leonardi-Bee, J., Al Khuwaitir, T.S., Al Mamun, A., Anovadiya, A.P., Azziz-Baumgartner, E., Báez, C., Bassetti, M., *et al.* (2014). Effectiveness of neuraminidase inhibitors in reducing mortality in patients admitted to hospital with influenza A H1N1pdm09 virus infection: a meta-analysis of individual participant data. Lancet Respir Med *2*, 395-404.

Pruijssers, A.J., George, A.S., Schäfer, A., Leist, S.R., Gralinksi, L.E., Dinnon, K.H., 3rd, Yount, B.L., Agostini, M.L., Stevens, L.J., Chappell, J.D., *et al.* (2020). Remdesivir Inhibits SARS-CoV-2 in Human Lung Cells and Chimeric SARS-CoV Expressing the SARS-CoV-2 RNA Polymerase in Mice. Cell Rep *32*, 107940.

Robbiani, D.F., Gaebler, C., Muecksch, F., Lorenzi, J.C.C., Wang, Z., Cho, A., Agudelo, M., Barnes, C.O., Gazumyan, A., Finkin, S., *et al.* (2020). Convergent antibody responses to SARS-CoV-2 in convalescent individuals. Nature *584*, 437-442.

Rogers, T.F., Zhao, F., Huang, D., Beutler, N., Burns, A., He, W.T., Limbo, O., Smith, C., Song, G., Woehl, J., *et al.* (2020). Isolation of potent SARS-CoV-2 neutralizing antibodies and protection from disease in a small animal model. Science *369*, 956-963.

Schäfer, A., Muecksch, F., Lorenzi, J.C.C., Leist, S.R., Cipolla, M., Bournazos, S., Schmidt, F., Maison, R.M., Gazumyan, A., Martinez, D.R., *et al.* (2021). Antibody potency, effector function, and combinations in protection and therapy for SARS-CoV-2 infection in vivo. J Exp Med *218*.

Schmidt, M.E., Knudson, C.J., Hartwig, S.M., Pewe, L.L., Meyerholz, D.K., Langlois, R.A., Harty, J.T., and Varga, S.M. (2018). Memory CD8 T cells mediate severe immunopathology following respiratory syncytial virus infection. PLoS Pathog *14*, e1006810.

Sheahan, T.P., Sims, A.C., Graham, R.L., Menachery, V.D., Gralinski, L.E., Case, J.B., Leist, S.R., Pyrc, K., Feng, J.Y., Trantcheva, I., *et al.* (2017). Broad-spectrum antiviral GS-5734 inhibits both epidemic and zoonotic coronaviruses. Sci Transl Med *9*.

Sheahan, T.P., Sims, A.C., Leist, S.R., Schäfer, A., Won, J., Brown, A.J., Montgomery, S.A., Hogg, A., Babusis, D., Clarke, M.O., *et al.* (2020a). Comparative therapeutic efficacy of remdesivir and combination lopinavir, ritonavir, and interferon beta against MERS-CoV. Nature Communications *11*, 222.

Sheahan, T.P., Sims, A.C., Zhou, S., Graham, R.L., Pruijssers, A.J., Agostini, M.L., Leist, S.R., Schäfer, A., Dinnon, K.H., 3rd, Stevens, L.J., *et al.* (2020b). An orally bioavailable broad-spectrum antiviral inhibits SARS-CoV-2 in human airway epithelial cell cultures and multiple coronaviruses in mice. Sci Transl Med *12*.

Wang, D., Hu, B., Hu, C., Zhu, F., Liu, X., Zhang, J., Wang, B., Xiang, H., Cheng, Z., Xiong, Y., *et al.* (2020). Clinical Characteristics of 138 Hospitalized Patients With 2019 Novel Coronavirus-Infected Pneumonia in Wuhan, China. Jama *323*, 1061-1069.

Wang, Z., Schmidt, F., Weisblum, Y., Muecksch, F., Barnes, C.O., Finkin, S., Schaefer-Babajew, D., Cipolla, M., Gaebler, C., Lieberman, J.A., *et al.* (2021). mRNA vaccine-elicited antibodies to SARS-CoV-2 and circulating variants. bioRxiv, 2021.2001.2015.426911.

Weinreich, D.M., Sivapalasingam, S., Norton, T., Ali, S., Gao, H., Bhore, R., Musser, B.J., Soo, Y., Rofail, D., Im, J., *et al.* (2020). REGN-COV2, a Neutralizing Antibody Cocktail, in Outpatients with Covid-19. New England Journal of Medicine.

Weisblum, Y., Schmidt, F., Zhang, F., DaSilva, J., Poston, D., Lorenzi, J.C., Muecksch, F., Rutkowska, M., Hoffmann, H.H., Michailidis, E., *et al.* (2020). Escape from neutralizing antibodies by SARS-CoV-2 spike protein variants. Elife *9*.

Williamson, B.N., Feldmann, F., Schwarz, B., Meade-White, K., Porter, D.P., Schulz, J., van Doremalen, N., Leighton, I., Yinda, C.K., Pérez-Pérez, L., *et al.* (2020). Clinical benefit of remdesivir in rhesus macaques infected with SARS-CoV-2. Nature *585*, 273-276.

Xu, Z., Shi, L., Wang, Y., Zhang, J., Huang, L., Zhang, C., Liu, S., Zhao, P., Liu, H., Zhu, L., *et al*. (2020). Pathological findings of COVID-19 associated with acute respiratory distress syndrome. The Lancet Respiratory Medicine *8*, 420-422.

Yang, X., Yu, Y., Xu, J., Shu, H., Xia, J., Liu, H., Wu, Y., Zhang, L., Yu, Z., Fang, M., *et al.* (2020). Clinical course and outcomes of critically ill patients with SARS-CoV-2 pneumonia in Wuhan, China: a single-centered, retrospective, observational study. Lancet Respir Med *8*, 475-481.

Zheng, S., Fan, J., Yu, F., Feng, B., Lou, B., Zou, Q., Xie, G., Lin, S., Wang, R., Yang, X., *et al.* (2020). Viral load dynamics and disease severity in patients infected with SARS-CoV-2 in Zhejiang province, China, January-March 2020: retrospective cohort study. Bmj *369*, m1443.

Zhou, F., Yu, T., Du, R., Fan, G., Liu, Y., Liu, Z., Xiang, J., Wang, Y., Song, B., Gu, X., *et al.* (2020a). Clinical course and risk factors for mortality of adult inpatients with COVID-19 in Wuhan, China: a retrospective cohort study. Lancet *395*, 1054-1062.

Zhou, P., Yang, X.L., Wang, X.G., Hu, B., Zhang, L., Zhang, W., Si, H.R., Zhu, Y., Li, B., Huang, C.L., *et al.* (2020b). A pneumonia outbreak associated with a new coronavirus of probable bat origin. Nature *579*, 270-273.

Zhu, N., Zhang, D., Wang, W., Li, X., Yang, B., Song, J., Zhao, X., Huang, B., Shi, W., Lu, R., *et al.* (2020). A Novel Coronavirus from Patients with Pneumonia in China, 2019. New England Journal of Medicine *382*, 727-733.

Zost, S.J., Gilchuk, P., Case, J.B., Binshtein, E., Chen, R.E., Nkolola, J.P., Schäfer, A., Reidy, J.X., Trivette, A., Nargi, R.S., *et al.* (2020a). Potently neutralizing and protective human antibodies against SARS-CoV-2. Nature *584*, 443-449.

Zost, S.J., Gilchuk, P., Chen, R.E., Case, J.B., Reidy, J.X., Trivette, A., Nargi, R.S., Sutton, R.E., Suryadevara, N., Chen, E.C., *et al.* (2020b). Rapid isolation and profiling of a diverse panel of human monoclonal antibodies targeting the SARS-CoV-2 spike protein. Nat Med *26*, 1422-1427.

Figure legends

Figure 1. The prophylactic and therapeutic efficacy of RDV against SARS-CoV-2 in mice.

(A) % starting weight in prophylactically treated mice with RDV at 12 hours before infection, and therapeutically at 12, 24, and 48 hours post infection.

(B) Lung viral titers in prophylactically and therapeutically treated mice with RDV.

(C) Lung discoloration score in prophylactically and therapeutically treated mice with RDV.

(D-E) Lung pathology in prophylactically and therapeutically treated mice with RDV.

(F) Pulmonary function in prophylactically and therapeutically treated mice with RDV. P values are from a 2-way ANOVA after correcting for multiple comparisons

Figure 2. The prophylactic and therapeutic efficacy of mAbs against SARS-CoV-2 in mice.

(A) % starting weight in prophylactically treated mice with C144 + C135 at 12 hours before infection, and therapeutically at 12, 24, and 48 hours post infection.

(B) Lung viral titers in prophylactically and therapeutically treated mice with C144 + C135.

(C) Lung discoloration score in prophylactically and therapeutically treated mice with C144 + C135.

(D-E) Lung pathology in prophylactically and therapeutically treated mice with C144 + C135.

(F) Pulmonary function in prophylactically and therapeutically treated mice with C144 + C135. P values are from a 2-way ANOVA after correcting for multiple comparisons

Figure 3. The therapeutic efficacy of RDV and mAbs as single agents and in combination at 24 hours post infection in SARS-CoV-2-infected mice.

(A) % starting weight in therapeutically treated mice with vehicle + HIV mAb, vehicle + C144 + C135, RDV + HIV mAb, and RDV + C144 + C135 at 24 hours post infection through day 12.

(B) % mortality in therapeutically treated mice with single agents and combination therapy.

(C) Lung discoloration score in therapeutically treated mice with single agents and combination therapy.

(D) Pulmonary function in therapeutically treated mice with vehicle + HIV mAb and RDV + C144 + C135. P values are from a 2-way ANOVA after correcting for multiple comparisons

Figure 4. The therapeutic efficacy of RDV and mAbs as single agents and in combination at 36 hours post infection in SARS-CoV-2-infected mice.

(A) % starting weight in therapeutically treated mice with vehicle + HIV mAb, vehicle + C144 + C135, RDV + HIV mAb, and RDV + C144 + C135 at 36 hours post infection.

(B) Day 3 post infection lung viral titers in therapeutically treated mice with single agents and combination therapy.

(C) Day 5 post infection lung viral titers in therapeutically treated mice with single agents and combination therapy.

(D) Lung discoloration scores in therapeutically treated mice with single agents and combination therapy.

(E) Pulmonary function in therapeutically treated mice with vehicle + HIV mAb and RDV + C144 + C135. P values are from a 2-way ANOVA after correcting for multiple comparisons

Supplemental figure legends

Figure S1. The prophylactic efficacy of mAb monotherapy against SARS-CoV-2 in mice treated at 12 hours before infection.

(A) % starting weight in therapeutically treated mice with C144, C135, or an HIV mAb at 12 hours before infection.

(B) Lung viral titers in therapeutically treated mice at 12 hours before infection.

(C) Lung discoloration score in therapeutically treated mice at 12 hours before infection.

(D-E) Lung pathology in therapeutically treated mice at 12 hours before infection. P values are from a 2-way ANOVA after correcting for multiple comparisons

Figure S2. The therapeutic efficacy of mAb monotherapy against SARS-CoV-2 in mice treated at 12 hours post infection.

(A) % starting weight in therapeutically treated mice with C144, C135, or an HIV mAb at 12 hours post infection.

(B) Lung viral titers in therapeutically treated mice at 12 hours post infection.

(C) Lung discoloration score in therapeutically treated mice at 12 hours post infection.

(D-E) Lung pathology in therapeutically treated mice at 12 hours post infection. P values are from a 2-way ANOVA after correcting for multiple comparisons

Figure S3. The therapeutic efficacy of mAb monotherapy against SARS-CoV-2 in mice treated at 24 hours post infection.

(A) % starting weight in therapeutically treated mice with C144, C135, or an HIV mAb at 24 hours post infection.

(B) Lung viral titers in therapeutically treated mice at 24 hours post infection.

(C) Lung discoloration score in therapeutically treated mice at 24 hours post infection.

(D-E) Lung pathology in therapeutically treated mice at 24 hours post infection. P values are from a 2-way ANOVA after correcting for multiple comparisons

Figure S4. The therapeutic efficacy of mAb monotherapy against SARS-CoV-2 in mice treated at 48 hours post infection.

(A) % starting weight in therapeutically treated mice with C144, C135, or an HIV mAb at 48 hours post infection.

(B) Lung viral titers in therapeutically treated mice at 48 hours post infection.

(C) Lung discoloration score in therapeutically treated mice at 48 hours post infection.

(D-E) Lung pathology in therapeutically treated mice at 48 hours post infection. P values are from a 2-way ANOVA after correcting for multiple comparisons

Figure S5. Lung pathology of SARS-CoV-2-infected mice treated with RDV and vehicle prophylactically and therapeutically.

Figure S6. Lung pathology of SARS-CoV-2-infected mice treated with C144 + C135 and an HIV mAb prophylactically and therapeutically.

Figure 1

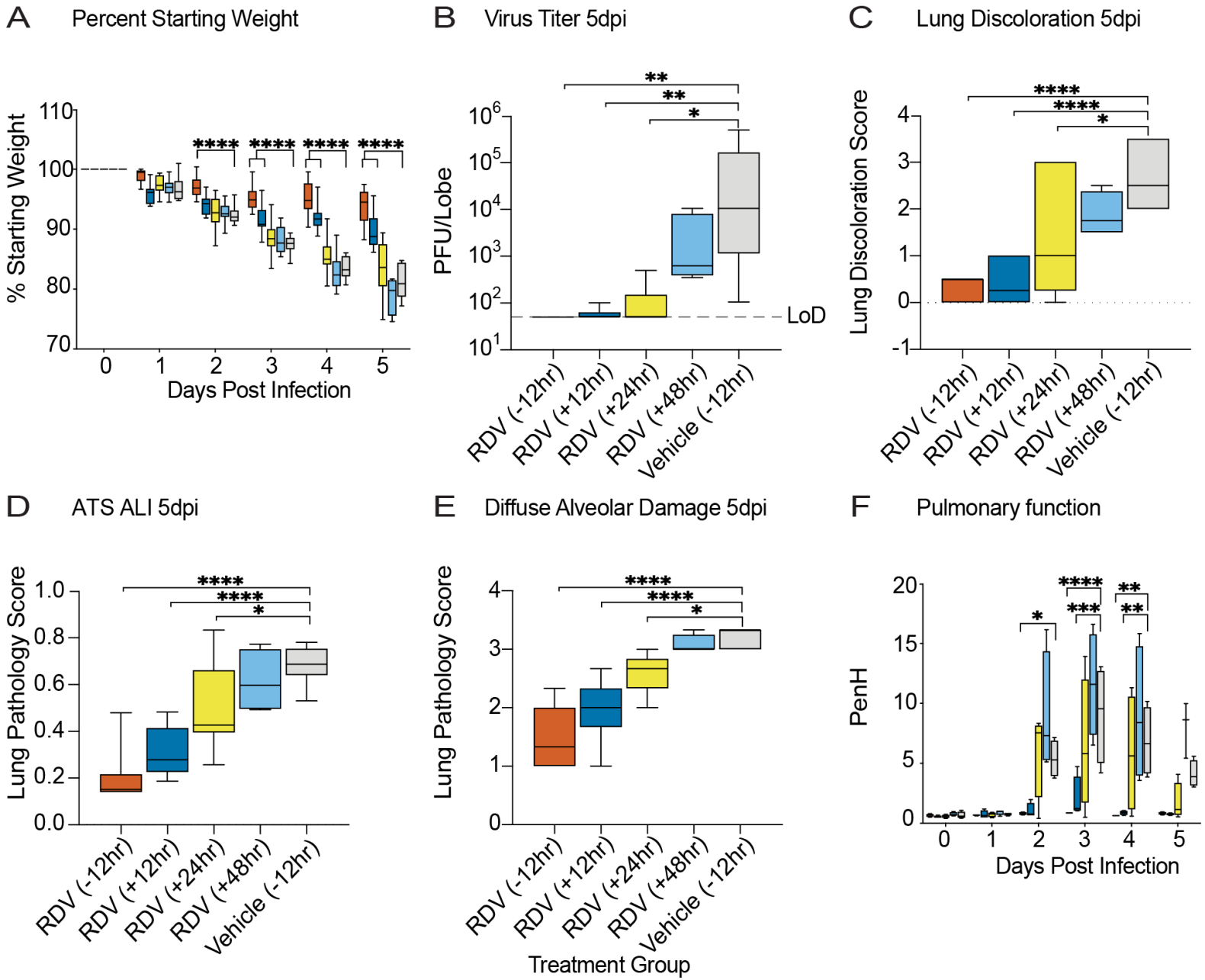
A
Percent Starting Weight
% Starting Weight
Days Post Infection
B
Virus Titer 5dpi
PFU/Lobe
LoD
C
Lung Discoloration 5dpi
Lung Discoloration Score
D
ATS ALI 5dpi
Lung Pathology Score
E
Diffuse Alveolar Damage 5dpi
Lung Pathology Score
Treatment Group
F
Pulmonary function
PenH
Days Post Infection
RDV (-12hr)
RDV (+12hr)
RDV (+24hr)
RDV (+48hr)
Vehicle (-12hr)

Figure 2

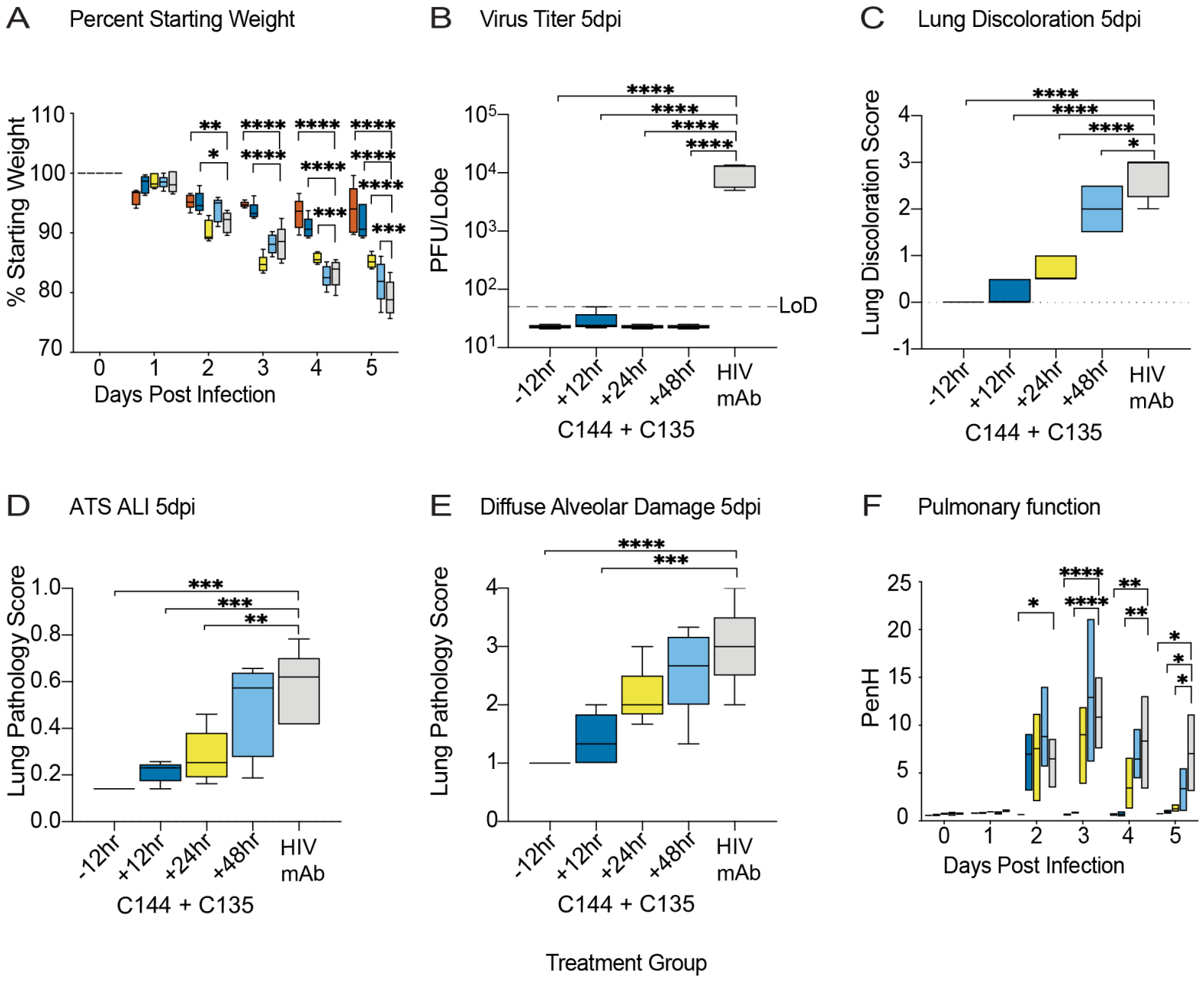
A
Percent Starting Weight
% Starting Weight
Days Post Infection
B
Virus Titer 5dpi
PFU/Lobe
LoD
C
Lung Discoloration 5dpi
Lung Discoloration Score
D
ATS ALI 5dpi
Lung Pathology Score
E
Diffuse Alveolar Damage 5dpi
Lung Pathology Score
F
Pulmonary function
PenH
Days Post Infection
-12hr
+12hr
+24hr
+48hr
HIV mAb
C144 + C135
Treatment Group

Figure 3

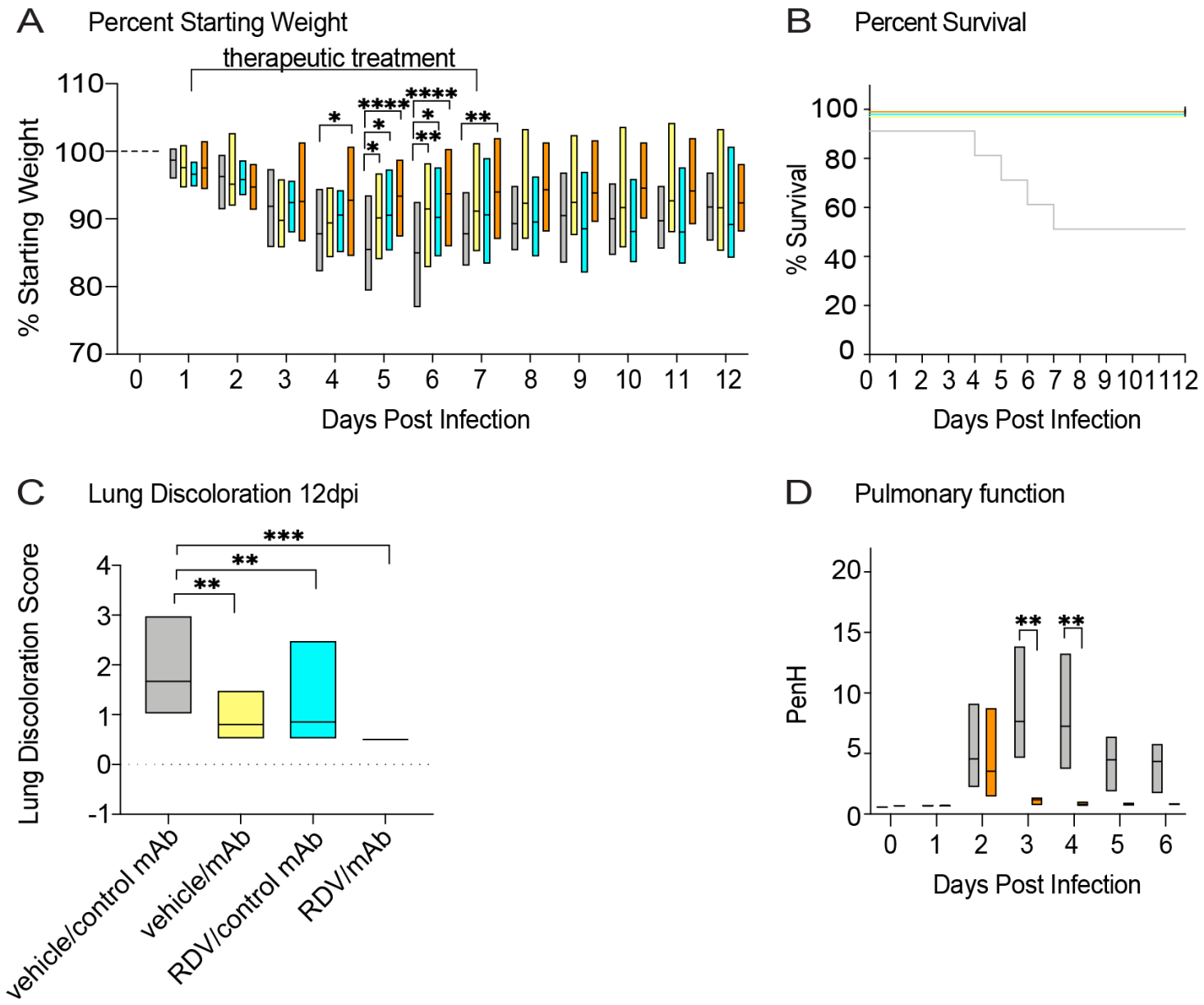
A
Percent Starting Weight
therapeutic treatment
% Starting Weight
110
100
90
80
70
0 1 2 3 4 5 6 7 8 9 10 11 12
Days Post Infection
B
Percent Survival
% Survival
100
80
60
40
20
0
0 1 2 3 4 5 6 7 8 9 10 11 12
Days Post Infection
C
Lung Discoloration 12dpi
Lung Discoloration Score
4
3
2
1
0
-1
vehicle/control mAb
vehicle/mAb
RDV/control mAb
RDV/mAb
D
Pulmonary function
PenH
20
15
10
5
0
0 1 2 3 4 5 6
Days Post Infection

Figure 4

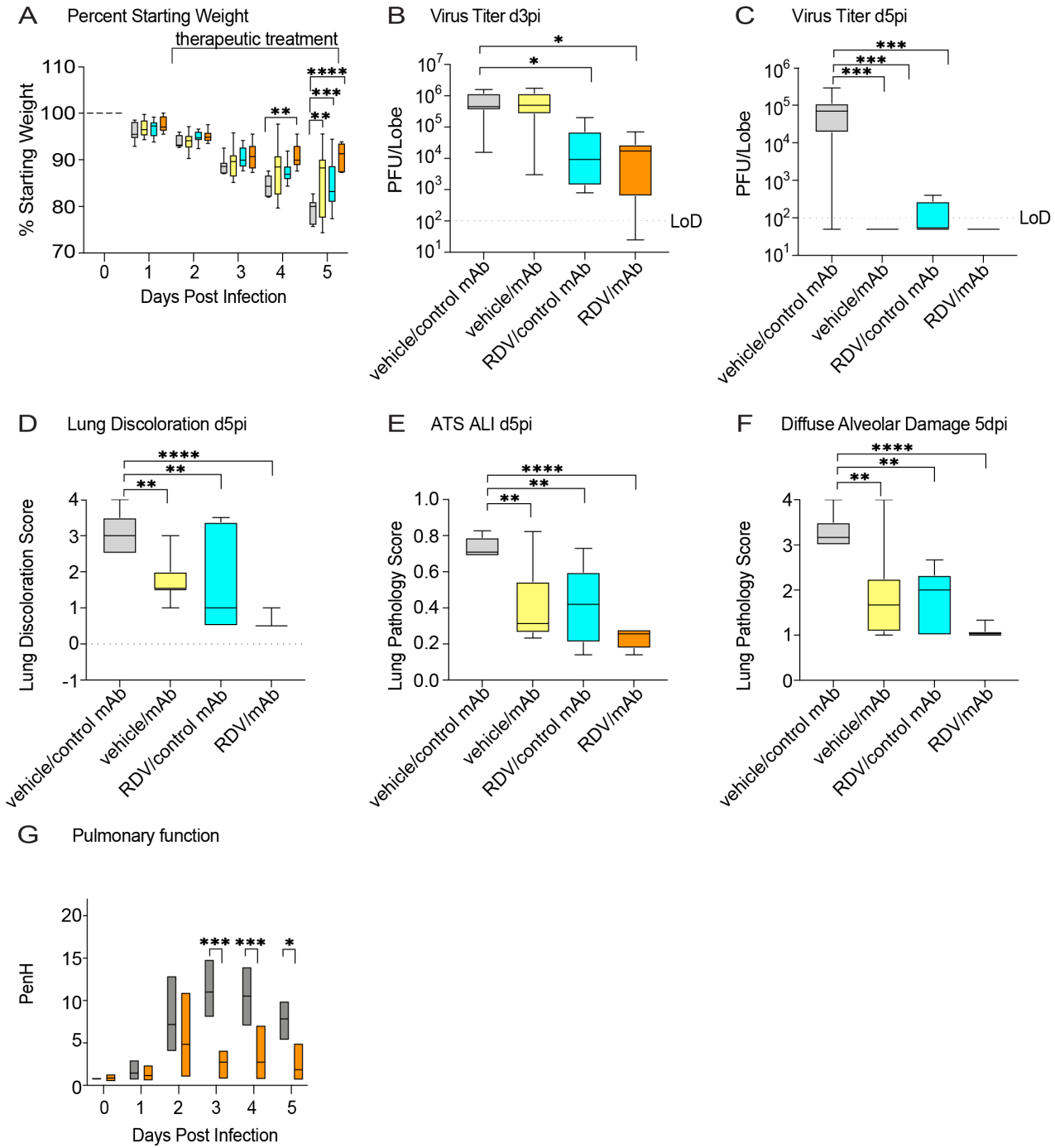
A
Percent Starting Weight
therapeutic treatment
% Starting Weight
Days Post Infection
B
Virus Titer d3pi
PFU/Lobe
LoD
vehicle/control mAb
vehicle/mAb
RDV/control mAb
RDV/mAb
C
Virus Titer d5pi
PFU/Lobe
LoD
D
Lung Discoloration d5pi
Lung Discoloration Score
E
ATS ALI d5pi
Lung Pathology Score
F
Diffuse Alveolar Damage 5dpi
Lung Pathology Score
G
Pulmonary function
PenH
Days Post Infection

Figure S1

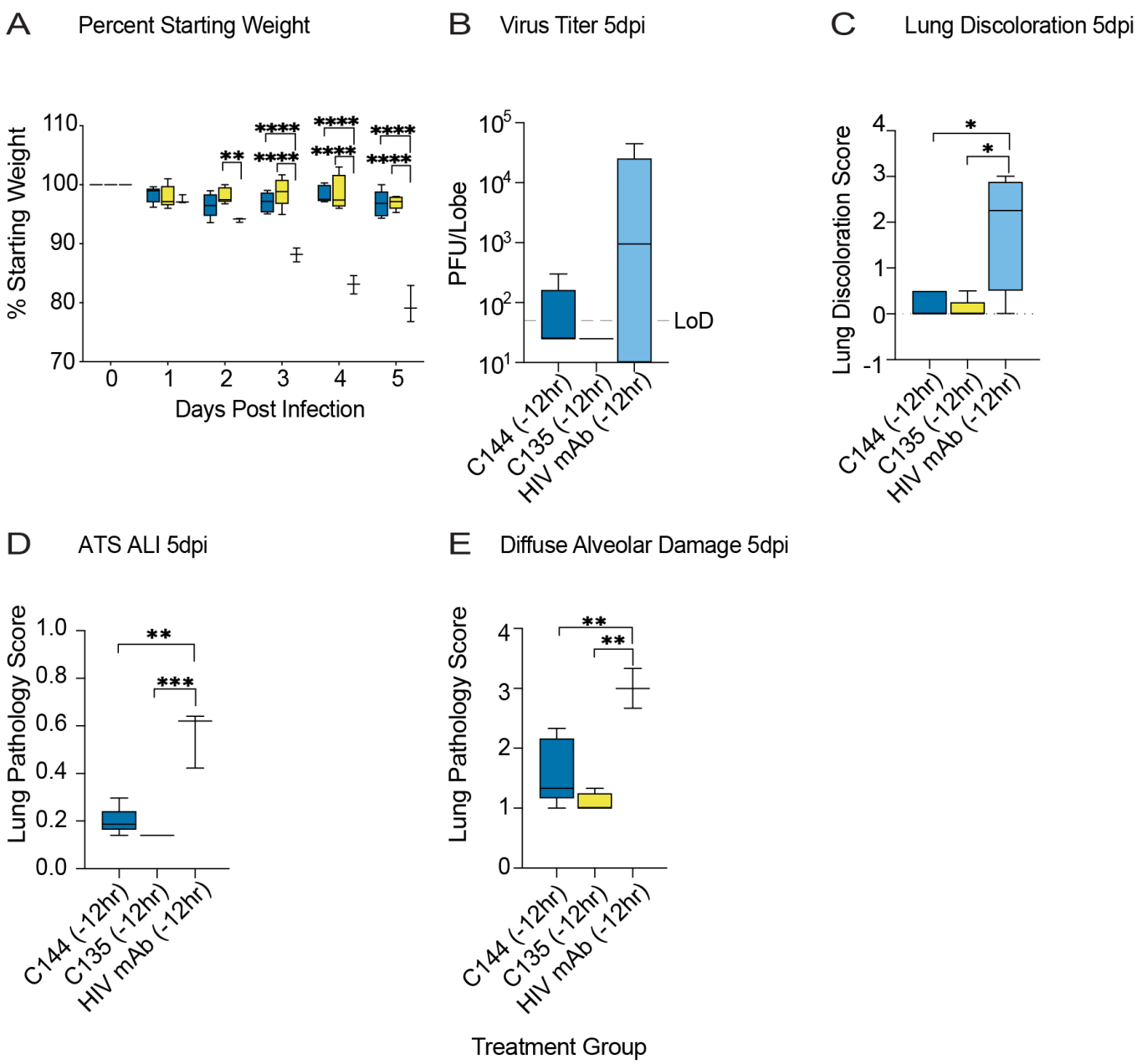
A
Percent Starting Weight
% Starting Weight
110
100
90
80
70
0
1
2
3
4
5
Days Post Infection
**
****
B
Virus Titer 5dpi
PFU/Lobe
10^5
10^4
10^3
10^2
10^1
LoD
C144 (-12hr)
C135 (-12hr)
HIV mAb (-12hr)
C
Lung Discoloration 5dpi
Lung Discoloration Score
4
3
2
1
0
-1
*
D
ATS ALI 5dpi
Lung Pathology Score
1.0
0.8
0.6
0.4
0.2
0.0
**
***
E
Diffuse Alveolar Damage 5dpi
Treatment Group

Figure S2

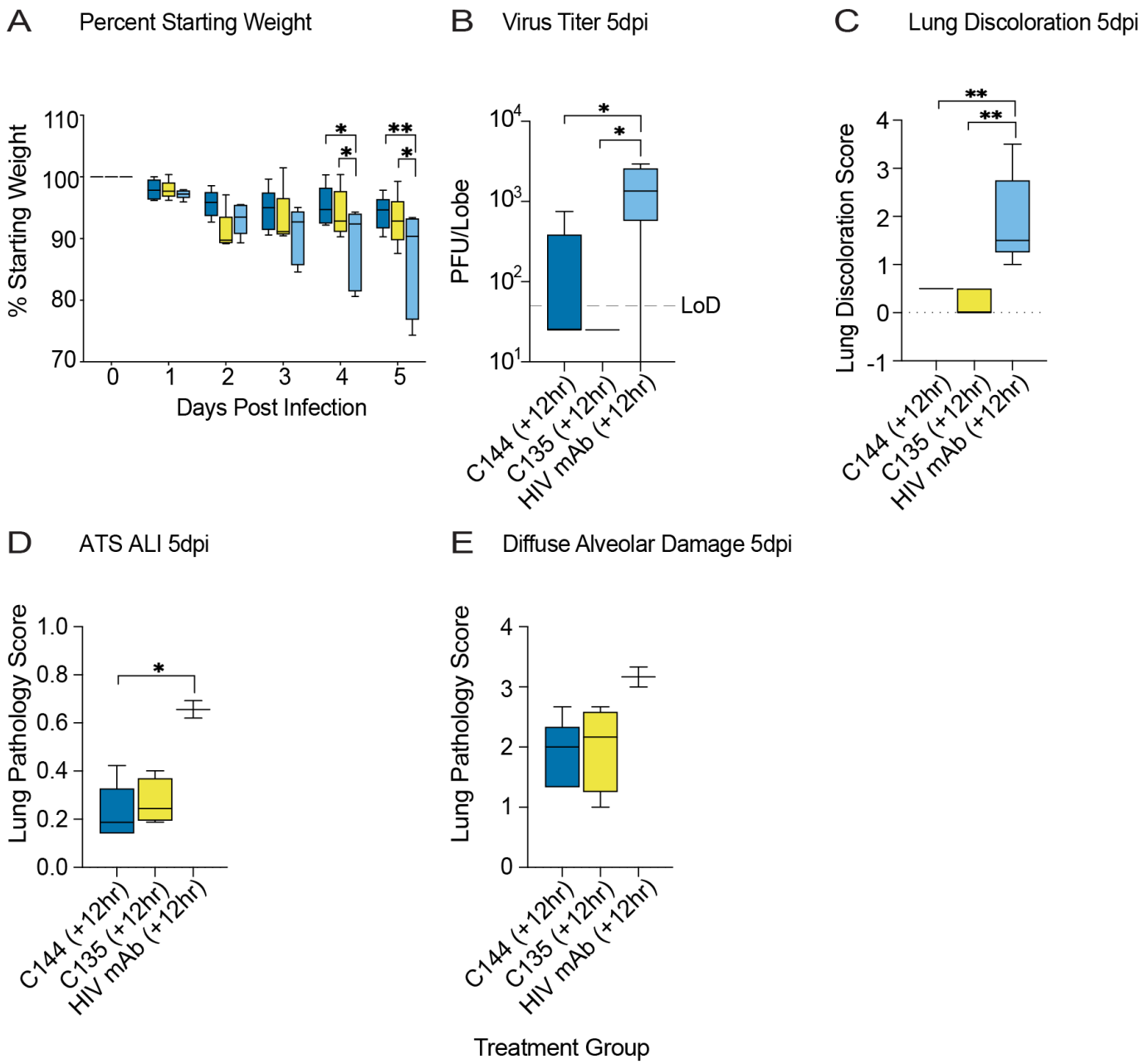
A
Percent Starting Weight
% Starting Weight
110
100
90
80
70
0
1
2
3
4
5
Days Post Infection
*
*
**
*
B
Virus Titer 5dpi
PFU/Lobe
10^4
10^3
10^2
10^1
LoD
*
*
C144 (+12hr)
C135 (+12hr)
HIV mAb (+12hr)
C
Lung Discoloration 5dpi
Lung Discoloration Score
4
3
2
1
0
-1
**
**
C144 (+12hr)
C135 (+12hr)
HIV mAb (+12hr)
D
ATS ALI 5dpi
Lung Pathology Score
1.0
0.8
0.6
0.4
0.2
0.0
*
C144 (+12hr)
C135 (+12hr)
HIV mAb (+12hr)
E
Diffuse Alveolar Damage 5dpi
Lung Pathology Score
4
3
2
1
0
C144 (+12hr)
C135 (+12hr)
HIV mAb (+12hr)
Treatment Group

Figure S3

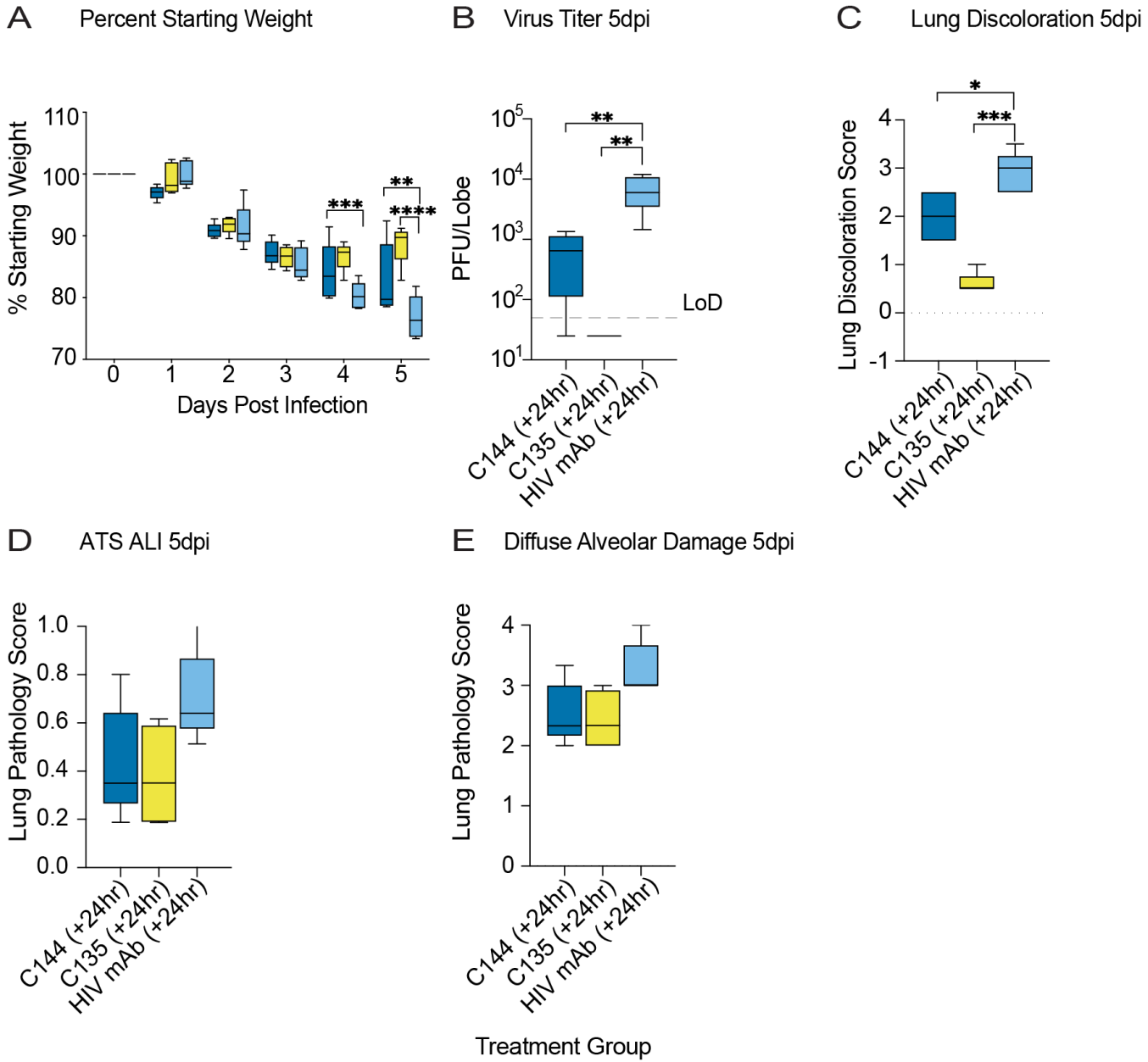
A
Percent Starting Weight
% Starting Weight
110
100
90
80
70
0
1
2
3
4
5
Days Post Infection
***
**
****
B
Virus Titer 5dpi
PFU/Lobe
10^5
10^4
10^3
10^2
10^1
LoD
**
**
C144 (+24hr)
C135 (+24hr)
HIV mAb (+24hr)
C
Lung Discoloration 5dpi
Lung Discoloration Score
4
3
2
1
0
-1
*
***
C144 (+24hr)
C135 (+24hr)
HIV mAb (+24hr)
D
ATS ALI 5dpi
Lung Pathology Score
1.0
0.8
0.6
0.4
0.2
0.0
C144 (+24hr)
C135 (+24hr)
HIV mAb (+24hr)
E
Diffuse Alveolar Damage 5dpi
Lung Pathology Score
4
3
2
1
0
C144 (+24hr)
C135 (+24hr)
HIV mAb (+24hr)
Treatment Group

Figure S4

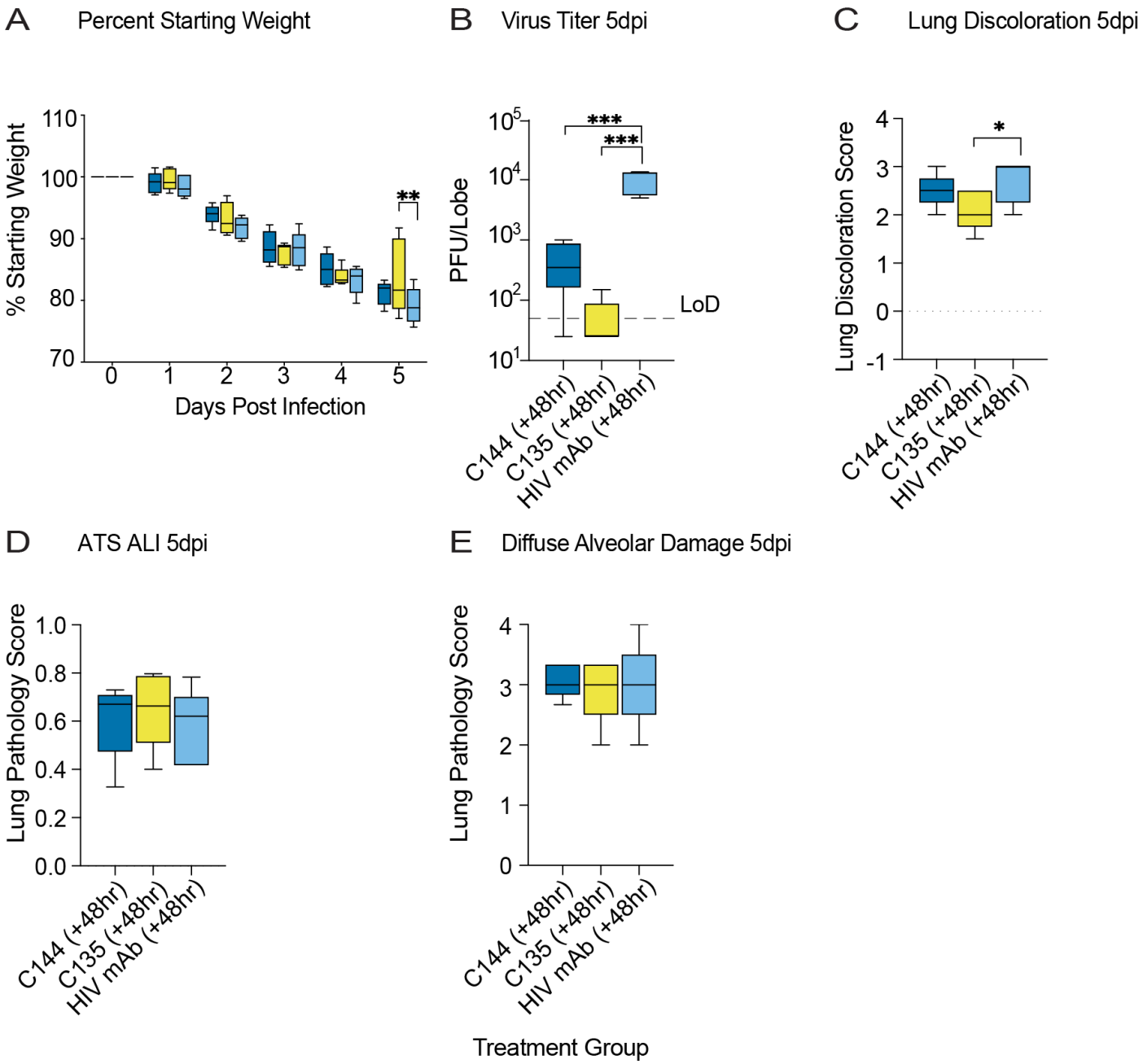
A
Percent Starting Weight
% Starting Weight
110
100
90
80
70
0
1
2
3
4
5
Days Post Infection
**
B
Virus Titer 5dpi
PFU/Lobe
10^5
10^4
10^3
10^2
10^1
***
***
LoD
C144 (+48hr)
C135 (+48hr)
HIV mAb (+48hr)
C
Lung Discoloration 5dpi
Lung Discoloration Score
4
3
2
1
0
-1
*
C144 (+48hr)
C135 (+48hr)
HIV mAb (+48hr)
D
ATS ALI 5dpi
Lung Pathology Score
1.0
0.8
0.6
0.4
0.2
0.0
C144 (+48hr)
C135 (+48hr)
HIV mAb (+48hr)
E
Diffuse Alveolar Damage 5dpi
Lung Pathology Score
4
3
2
1
0
C144 (+48hr)
C135 (+48hr)
HIV mAb (+48hr)
Treatment Group

Figure S5

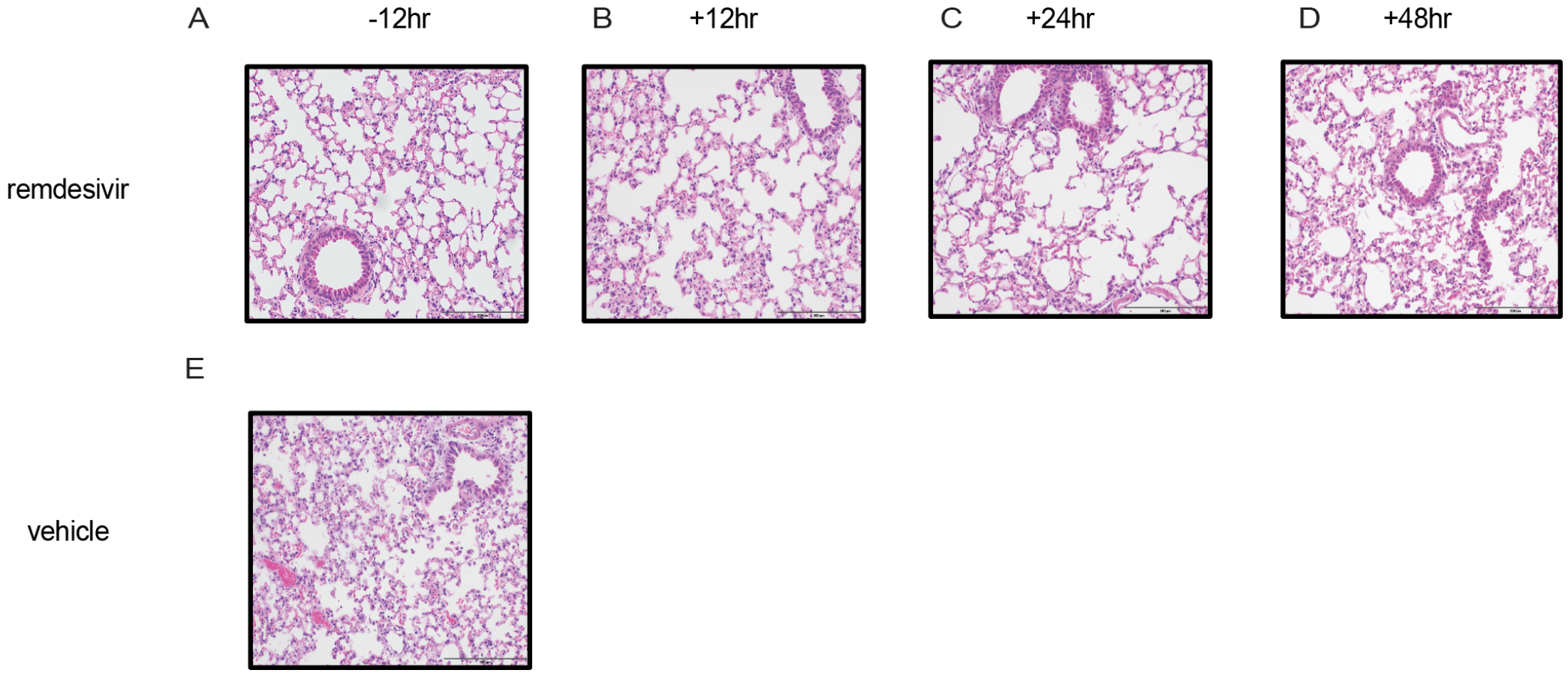

Figure S6

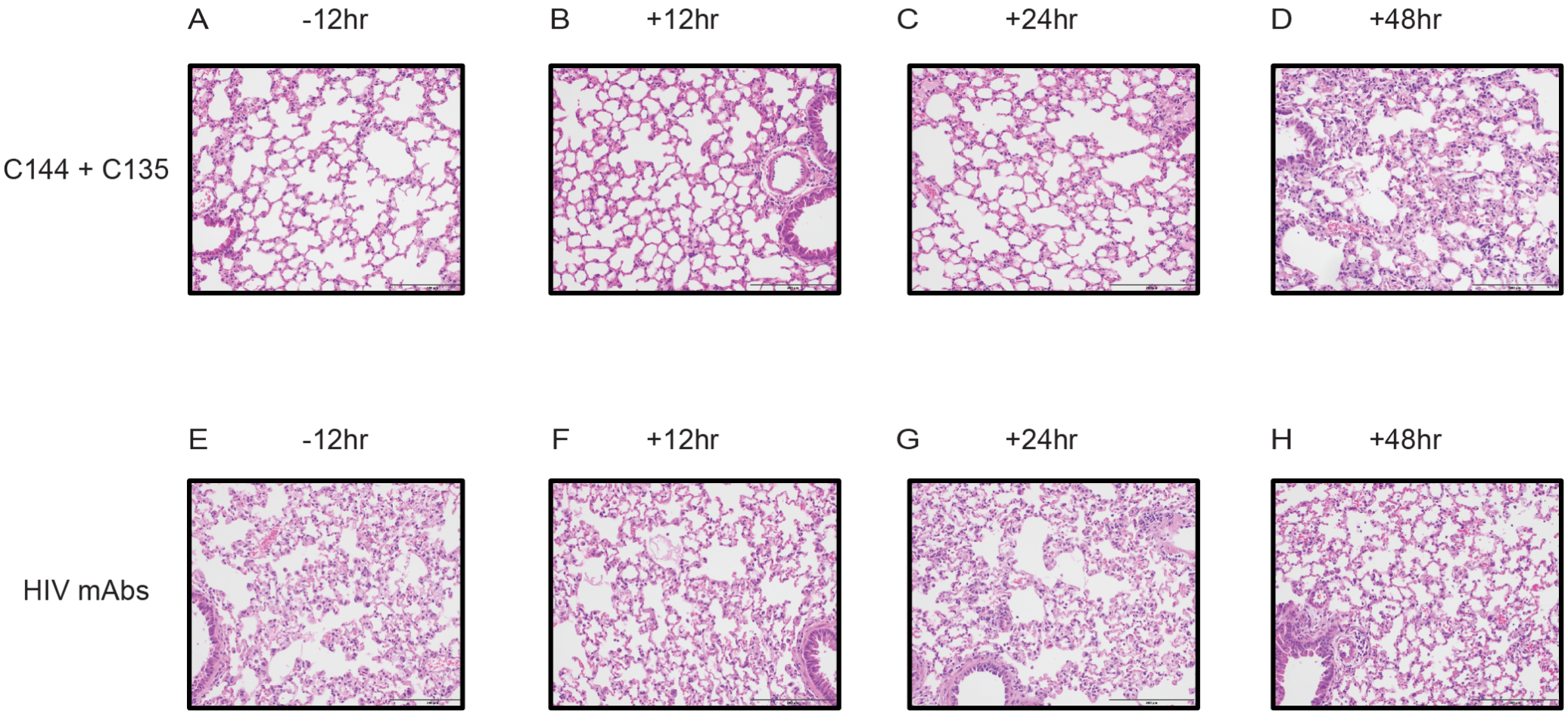
A -12hr
B +12hr
C +24hr
D +48hr
C144 + C135
E -12hr
F +12hr
G +24hr
H +48hr
HIV mAbs